

## Dynamic Buckling Analysis of Ductile Damage Evolution for Thin Shell With Lemaitre's Model

Iheb Hammar <sup>1\*</sup>, Mohamed Djermane <sup>1</sup>, Belkacem Amieur <sup>1</sup>

<sup>1</sup> FIMAS Lab, Department of Civil Engineering, Tahri Mohamed University, Bechar, 08000 Algeria.

Received 05 October 2023; Revised 12 February 2024; Accepted 17 February 2024; Published 01 March 2024

### Abstract

Thin-shell structures are used in several fields of construction and are often exposed to severe dynamic environments, making them susceptible to dynamic instabilities. These instabilities are typically preceded by varying degrees of damage to the shell, justifying the need to incorporate this behavior in the formulation of the finite elements used. The objective of this work is to evaluate the different dynamic instability criterion in the presence of damage, afterward, evaluate the influence of this behavior on the stability of shells subjected to the dynamic excitations. The methodology of this project is essentially numerical, based on the finite element method. We are asked to program the introduction of damaging behavior and Lemaitre's model criteria in the DYNCOQ program developed locally. To examine the results, two examples extracted from the literature were presented. The first model aimed to confirm the proper functioning of the program and the convergence of the plasticity criterion (Lemaitre's model). As for the second model, it allows us to test the dynamic instability. A comparison was made with experimental data from previously published literature, revealing a strong agreement between the calculated and experimental results. The obtained results prove the utility of considering this behavior in the shell analysis.

*Keywords:* Dynamic Buckling; Shells; Damage; Finite Element; Imperfections; Damage Measurement.

### 1. Introduction

The field of continuum damage mechanics was initially pioneered by McClintock (1968) [1] and has since been actively pursued by researchers, such as a ductile damage model for ductile rupture, founded on void nucleation and growth was initially offered by Gurson (1977) [2]. In this criterion, the process of creating microvoids, growth, and coalescence was taken into account by a yield surface function and an upper bound approach of a hollow sphere made of ideal plastic von Mises material. The proposed yield surface could not represent the coalescence and fracture of material due to the low growth rate of microvoids. Tvergaard and Needleman modified the original yield surface and developed a constitutive model for porous metal plasticity, named the Gurson-Tvergaard-Needleman (GTN) criterion [3]. Another well-known standard, Lemaitre's ductile damage criterion, was initially offered by Lemaitre (1985) [4]. This formulation describes the evolution of irreversible phenomena such as the growth of voids under plastic deformations by the effective stress concept. The significant advantage of this criterion is that only one material dependent damage parameter is required for each material. The damage models introduced by these researchers have gained widespread acceptance and application in the finite element method (FEM). The application of these models on the shells guided us to the work of Lee & Pourboghrat (2005) [5]. The latter has proposed a numerical simulation of the Punchless Piercing Process using Lemaitre's model. The same model was used with the tavelgard models in the work of He et al. (2020) [6].

\* Corresponding author: [iheb.hammar@univ-bechar.dz](mailto:iheb.hammar@univ-bechar.dz)

 <http://dx.doi.org/10.28991/CEJ-2024-010-03-012>



© 2024 by the authors. Licensee C.E.J, Tehran, Iran. This article is an open access article distributed under the terms and conditions of the Creative Commons Attribution (CC-BY) license (<http://creativecommons.org/licenses/by/4.0/>).

While the plastic damaging behavior is well-documented in tensile tests, as evidenced by the research of Li et al. (2024) [7], Laboubi et al. (2023) [8], and Restrepo et al. (2018) [9], Similarly, in compression, the crack closure effect has been examined in the model proposed by De Souza Neto (2002) [10], with a concise explanation provided by Shamshiri et al. (2023) [11]. However, there is a notable scarcity of research focusing on the dynamic testing of this behavior. In this study, we employed finite element formulations, placing particular emphasis on the stress update procedure involving von Mises plasticity and the Lemaitre isotropic damage model. The primary objective was to investigate the evolution of material responses and damage progression while also predicting critical load demands. This approach enables subsequent comparisons and facilitates insights into the practical significance of this behavior.

In the literature, several researchers are studying the dynamic instabilities of thin shells [12-14], for example, treated dynamic buckling of thin shells in seismic zones, then succeed by Amieur (2019) [15] and Amieur et al. (2023) [16] with the Dynamic buckling analysis of functionally graded materials. This work essentially presents our benchmark in validating the numerical example presented in the next paper.

### 1.1. Theoretical Presentation of the Instability Issue

The analysis of the stability problem is primarily governed by the choice of stability criteria. In 1788, Lagrange proposed a criterion, subsequently known as the "energy criterion" for conservative discrete systems. According to this criterion, the necessary and sufficient condition for such a system to be in stable equilibrium is that its potential energy exhibits a local minimum for that state. If this energy is at a maximum, the equilibrium is unstable. Based on linearization through asymptotic developments and thus applicable to infinitely small movements, this criterion has been criticized and extended to bounded perturbations by Dirichlet (1846) [17]. This criterion does not apply to dynamic cases, non-conservative loadings, or large displacements. Even when respecting these limitations, the Lagrange-Dirichlet criterion remains subject to numerous criticisms as it is, in fact, not based on any rigorous definition of stability.

### 1.2. The Significance of Stability According to Lyapunov

In 1907, Lyapunov provided a precise definition of stability [18], along with the methods and fundamental results that subsequent research has referred to. Under certain conditions, according to Lyapunov's stability sense, the energy criterion constitutes a necessary but not sufficient condition for continuous static systems. According to Lyapunov, an equilibrium configuration of a system is stable if any solution to the nonlinear equations of motion, starting at time  $t=0$  from a configuration sufficiently close to  $U_0$  with low velocity, remains arbitrarily close to the  $U_0$  configuration for all subsequent values of  $t$ . The term "sufficiently close configuration to  $U_0$ " is achieved through a small transient perturbation. Such a perturbation could be created by applying a small parasitic force to the system for a brief moment.

### 1.3. Practical Criteria for Dynamic Buckling

Researchers in the domain of dynamic instability primarily depend on three criteria to investigate critical conditions in structures subjected to dynamic loads. These criteria are: the Budiansky-Roth criterion, also known as the equation of motion resolution criterion; the phase plane criterion of total potential energy Hoff and Bruce (1953) [19], and the total potential energy criterion Simitses (1966) [20]. The first two criteria are the focus of our work and will be briefly defined. It is worth noting that the use of catastrophe theory (Raftoyiannis et al. (2006) [21], and Bamberger (1981) [22]) has also been attempted in the analysis of dynamic instability. This approach has not received much attention from researchers and will not be presented in what follows. More recently, other criteria derived from the energy method with modifications have been proposed by Kounadis and Raftoyiannis (1990) [23], Koimadis (1991) [24], Koimadis (1996) [25], and Kounadis et al. (1999) [26]. These criteria are applications of the energy criterion and are still limited to simple structures (1 or 2 degrees of freedom), and do not seem to have practical significance thus far.

#### *Budiansky and Ruth Criterion*

The first and most common stability criterion is due to Budiansky (1962) [27]. It has been framed as an engineering application of Liapounov's stability criteria. In this criterion, the time displacement curve is plotted for several values of the applied load. The load value corresponding to a curve that yields a "jump" relative to its neighboring curves indicates the critical dynamic buckling value.

This criterion, originally introduced by Budiansky (1962) [27] and by Budiansky (1967) [28], which can be interpreted as an application of stability in the sense of Lyapunov, is the most commonly used in practice.

#### *Phase Plane Criterion*

The curve representing the movement is plotted in phase plan. Stable movements are characterized by limited trajectories and do not move too much away from the solution of the static equilibrium, which plays the role of a center of attraction. As the load reaches the critical value, the trajectory moves away from that pole with no oscillation around it.

### 1.4. Lemaitre's Model

Within this section, we present an algorithm that integrates the elasto-plastic-damage model according to Lemaitre's theory, incorporating a modified hardening law, specifically a saturation stress. This algorithm is influenced by the research of Lee & Pourboghrat (2005) [5]. The process entails determining the state variables of constitutive equations through a predictive elastic and corrective plastic step. Additionally, the  $J_2$  plasticity theory was combined with the continuum damage mechanics (CDM) criteria. The time interval of study is denoted as  $[0, T]$ , and  $\Delta \epsilon$  represents the required strain increment to update the variables at time  $t_{(i+1)}$ . At  $t_{(i)}$ , the values of stress  $\sigma_{(i)}$ , plastic strain  $\epsilon_{(i)}^{pl}$ , and the damage parameters  $D_{(i)}$  are known. Assuming additive rule, the strain increment,  $\Delta \epsilon$ , is defined into elastic increment  $\Delta \epsilon^{el}$  and plastic increment  $\Delta \epsilon^{pl}$  given by,  $\Delta \epsilon = \Delta \epsilon^{el} + \Delta \epsilon^{pl}$ . For the elastic trial state  $\Delta \epsilon^{pl} = 0$ , the elastic Hooke's law coupled with the damage is computed from [1].

$$\sigma^{trial} = \sigma_{(i)} + (1 - D_{(i)}) (\lambda \text{trace}(\Delta \epsilon) I + 2\mu \Delta \epsilon) \tag{1}$$

where  $\sigma^{trial}$  represents the elastic predictor,  $\lambda$  and  $\mu$  are Lamé's constants, and  $I$  is the identity matrix. Subsequently, the yield surface is examined using Equation 2 to determine whether the trial stress falls within the elastic domain. The trial deviatoric component of the stress tensor  $S^{trial}$ , is defined according to Equation 2.

$$\Phi^{trial} = \frac{[3J_2(S^{trial})]^{1/2}}{1 - D_{(i)}} - \sigma_y(\underline{\epsilon}_{(i)}^{pl}) \tag{2}$$

$$S^{trial} = \sigma^{trial} - \frac{1}{3} \text{trace}(\sigma^{trial}) I \tag{3}$$

If the yield condition  $\Phi^{trial} \leq 0$  is satisfied, there is no plastic behavior or damage evolution, and the state variables are updated as trial values at  $t_{(i+1)}$ .

$$\underline{\epsilon}_{(i+1)}^{pl} = \underline{\epsilon}_{(i)}^{pl}, D_{(i+1)} = D_{(i)}, \sigma_{(i+1)} = \sigma_{(i)} \tag{4}$$

Alternatively, if the yield condition  $\Phi^{trial} \leq 0$  is not satisfied, the process is considered to be elasto-plastic, and the plastic corrector step should be employed to calculate the plastic strain. Equation 2 must fulfill the consistency condition  $\Phi = 0$  by utilizing the trial deviatoric stress in order to describe plastic flow. This condition ensures that the updated deviatoric stress  $S_{(i+1)}^{trial}$  lies on the yield surface.

$$S_{(i+1)} = R_{(i+1)} q \tag{5}$$

where  $q$  represents the radial direction for the plastic correction, which needs to fulfill the hardening isotropic condition, denoted as:

$$q = \frac{S^{trial}}{|S^{trial}|} = \frac{S_{(i+1)}}{|S_{(i+1)}|} \tag{6}$$

and  $R_{(i+1)}$  is the radius of the yield surface at time  $t_{(i+1)}$  obtained by:

$$R_{(i+1)} = \sqrt{\frac{2}{3}} (1 - D_{(i+1)}) k_{(i+1)} \tag{7}$$

$$R_{(i+1)} = \sqrt{\frac{2}{3}} R_v \left( 1 - D_{(i)} - \sqrt{\frac{2}{3}} \alpha_{(i)} \Delta \gamma \right) \tag{8}$$

where;

$$R_v = \frac{2}{3} (1 + \vartheta) + 3(1 - 2\vartheta) \left( \frac{\sigma_h}{S} \right)^2 \tag{9}$$

$$\alpha_{(i)} = \frac{\sigma_{\epsilon q}^2 R_v}{2ES(1 - D)^2} \tag{10}$$

where  $\vartheta$  is the Poisson ratio,  $\sigma_h$  is the hydrostatic stress tensor,  $S$  is the Von Mises equivalent stress.

In this research, a distinct hardening law was utilized in contrast to the original algorithm. Equation (11) incorporated the Voce-type saturation law. Consequently, the hardening modulus  $h_n = d\sigma_{y,(i)} / d\underline{\epsilon}_{(i)}^{pl}$  at the instance  $i$  is defined as follows:

$$\sigma_{y,(i)} = \sigma_{y0} + \sigma_{sat} (1 - \exp(-w \times \underline{\epsilon}_{(i)}^{pl})) \tag{11}$$

being  $\sigma_{sat}$  and  $S_{(i+1)}$  the material parameters, from Equation 2, can be represented by:

$$S_{(i+1)} = S^{trial} - 2\mu(1 - D_{(i)}) \Delta \gamma q \tag{12}$$

Taking Equations 1, 5, and 12, we obtained the next expression that leads to a second-order equation with respect to  $\Delta\gamma$ .

$$A\Delta\gamma^2 + B\Delta\gamma + C = 0 \tag{13}$$

where;

$$A = \alpha_{(i)}h_{(i)} \tag{14}$$

$$B = \alpha_{(i)}\sigma_{y,(i)} - (1 - D_{(i)})(h_{(i)} + 3G) \tag{15}$$

$$C = S^{trial} - \sigma_{y,(i)}(1 - D_{(i)}) \tag{16}$$

The two roots computed of Equation 13 should satisfy the following constrains:

$$\Delta\gamma = (\Delta\gamma_{(j)}), \Delta\gamma > 0, j = 1,2 \tag{17}$$

Solving second-order equation, we obtained the plastic corrector ( $\Delta\gamma$ ), which is used to update the state variables at  $t_{(i+1)}$ .

$$\sigma_{(i+1)} = \sigma^{trial} - 2\mu(1 - D_{(i)})\Delta\gamma q \tag{18}$$

$$\bar{\epsilon}_{(i+1)}^{pl} = \bar{\epsilon}_{(i)}^{pl} + \sqrt{\frac{2}{3}}\Delta\gamma \tag{19}$$

$$D_{(i+1)} = D_{(i)} + \sqrt{\frac{2}{3}}\Delta\alpha_{(i)}\Delta\gamma \tag{20}$$

Figure 1 represented the Flowchart algorithm above for the standard Lemaitre’s ductile damage model of Lee & Pourboghraat (2005) [5].

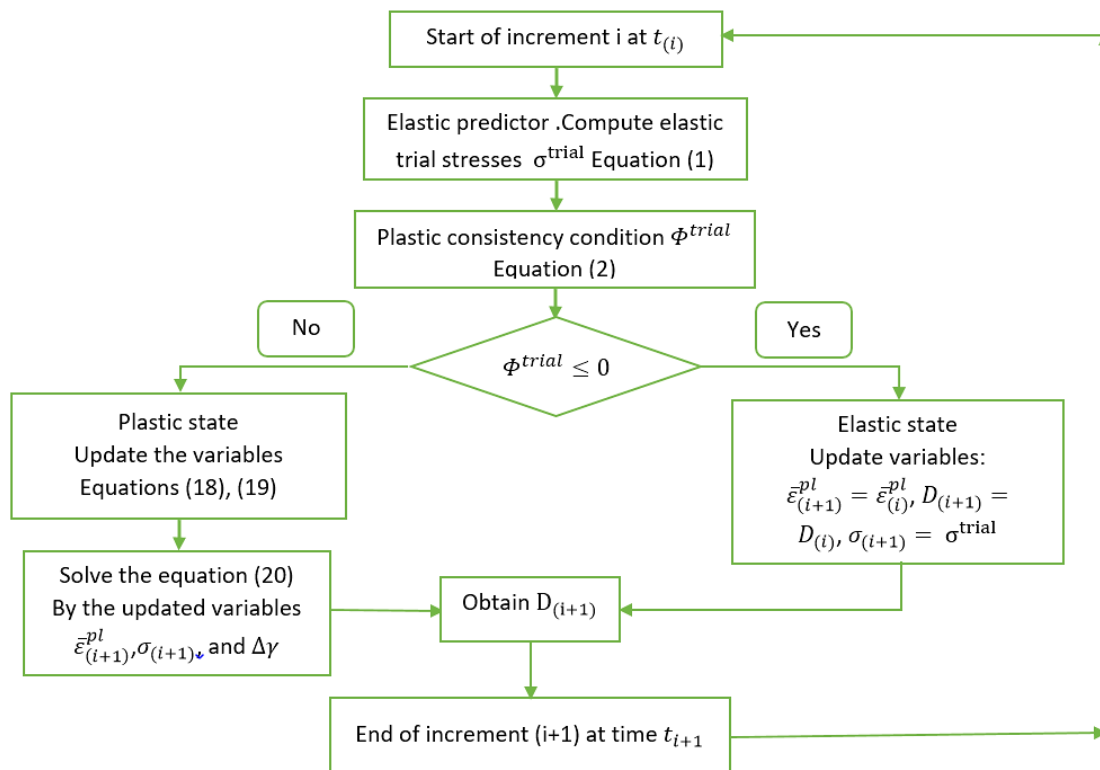


Figure 1. the Flowchart algorithm for the standard Lemaitre’s damage model

The algorithm above was initially introduced by Lee & Pourboghraat (2005) [5]. It has been used repeatedly by various researchers, taking Anduquia-Restrepo et al. (2018) [9] as an example. In this work, a numerical analysis of damage evolution for a simple tensile test of Dual-Phase steel is studied. Simulations were conducted using the finite element code ABAQUS/Explicit through a VUMAT subroutine to implement Lemaitre's model. To ensure the proper functioning of the model, we simulated the example presented by Restrepo.

Figure 2 shows the comparison of the results of the curves obtained from the Restrepo simulation and load-unload tensile experiment tests with the model proposed in this work. In order to simulate exactly the same geometry and mesh, we used the geometric coordinates from an Abaqus input file similar to the Restrepo example. The obtained result confirms the good agreement between the two models and demonstrates a very close convergence to the experimental results.

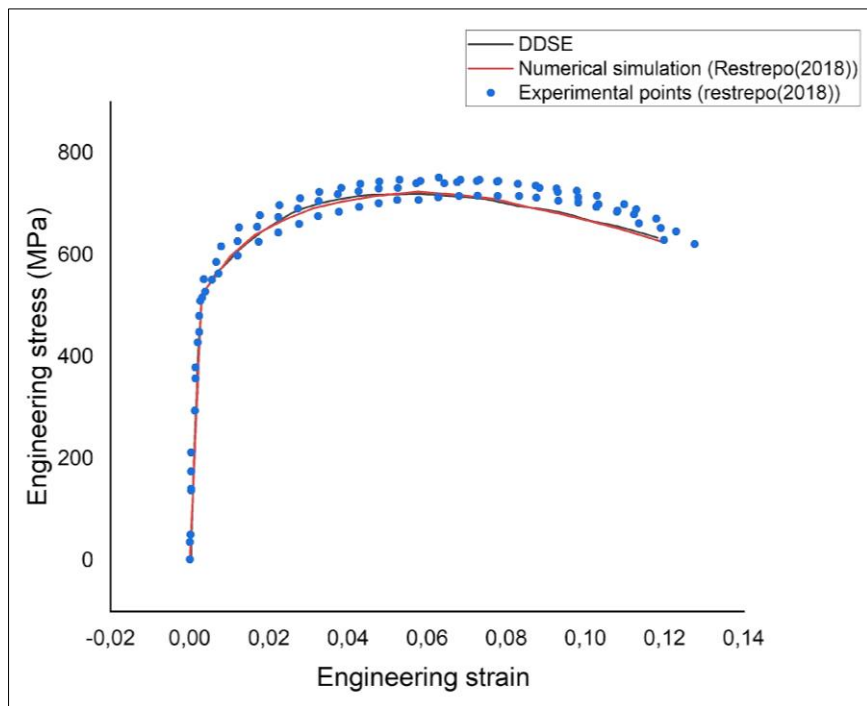


Figure 2. Comparison of engineering stress-strain tensile test

## 2. Numerical Application

### 2.1. Spherical Cap shallow Example

This widely recognized example has been examined by numerous authors employing various approaches, including Saigal and Yang (1985) [29], Nagarajan and Popov (1974) [30], and Bathe et al. (1975) [31]. In this instance, the goal is to calculate the transient response of an elastic-plastic, shallow spherical shell subjected to uniform pressure. The geometric and mechanical details of the problem are presented in Figure 3 and Table 1. It is assumed that the material follows the Von Mises criterion with isotropic hardening. A step-type pressure of 600 psi is applied to induce elastic-plastic behavior.

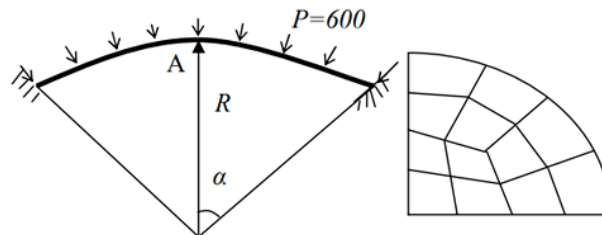


Figure 3. Spherical cap: geometry and mesh

Table 1. Geometrical and material properties

Properties	Symbol	Value
radius	R	22.7 in
thickness	e	0.41 in
Young modulus	E	$10.5 \times 10^6$ psi
Poisson ratio	$\nu$	0.3
yield	$\sigma_0$	2400 psi
Density	$\rho$	$2.45 \times 10^{-4}$ lb-sec <sup>2</sup> /in <sup>4</sup>

The various analyses conducted are presented in Figures 4 and 5. which indicates the agreement of the results obtained with those published in previous references. Furthermore, one can conclude that:

- Damping of the peak. The differences between two successive peaks in the elastic and elastic-plastic analyses are  $141.19 \times 10^{-3}$  inches and  $60.15 \times 10^{-3}$  inches, respectively. The reason is the damping caused by the repeated process of elastic unloading and plastic loading.
- Elongation of the period due to nonlinear softening

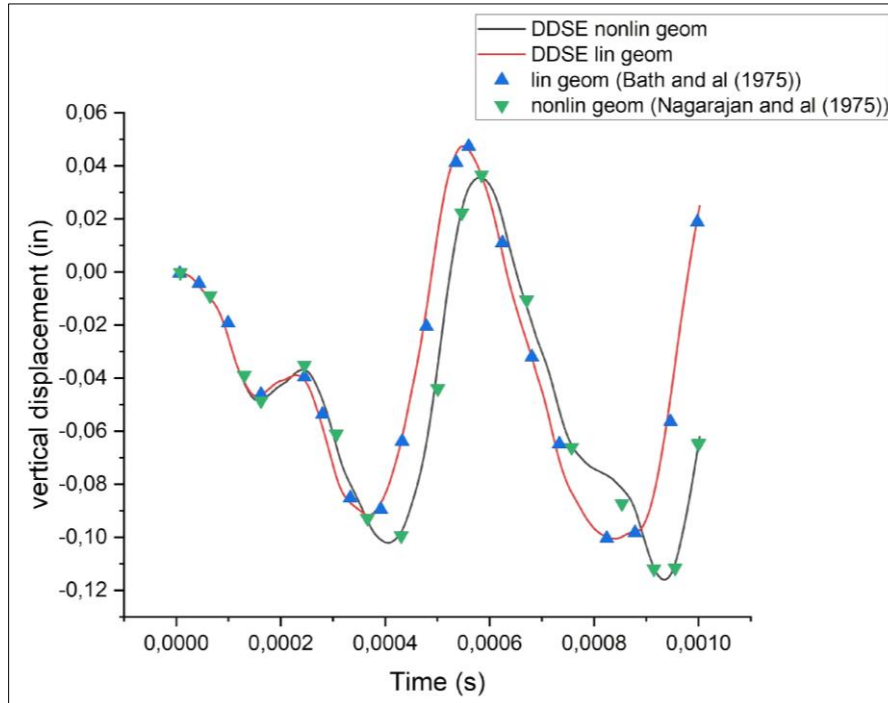


Figure 4. Elastic spherical cap displacement: comparison of results

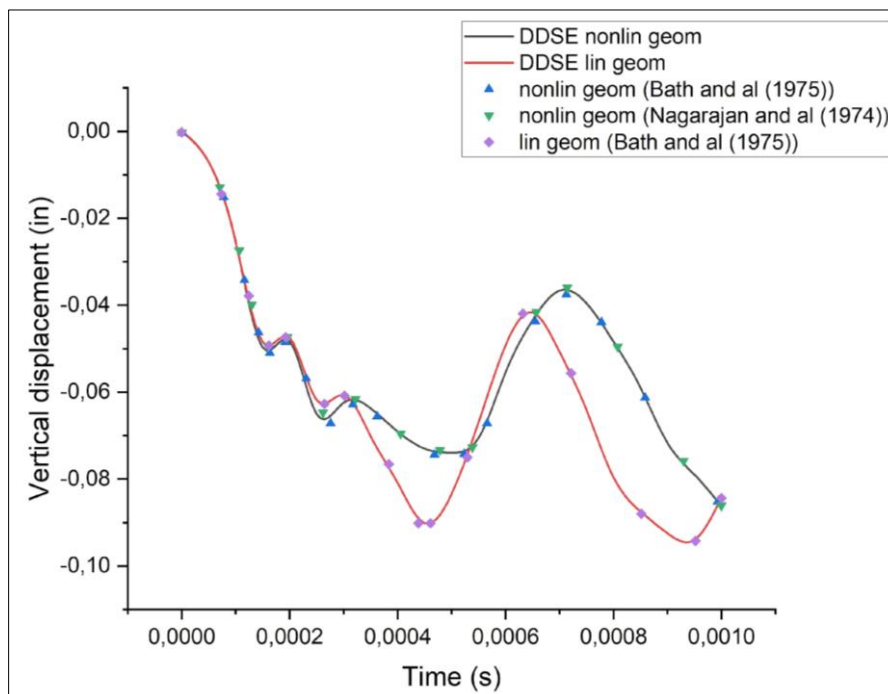


Figure 5. Elasto-plastic spherical cap displacement: comparison of results

### 2.2. Cylindrical Panel Example

This example is used for the first time in dynamic stability, according to Djermame (2007) [12], Djermame et al. (2007) [32], and subsequently Djermame et al. (2014) [14], Amieur et al. (2019) [15], and Amieur et al. (2023) [16] for isotropic materials.

To study this effect, we considered a mesh of  $(2 \times 2)$  for the time increment  $\Delta t = 1E-06$  (s). The panel shown in Figure 6 is subjected to a distributed step pressure  $P$ , the sample geometry was modelled using 3D eight-node brick elements with an integration point. Geometrical and material properties details of the problem are presented and Table 2.

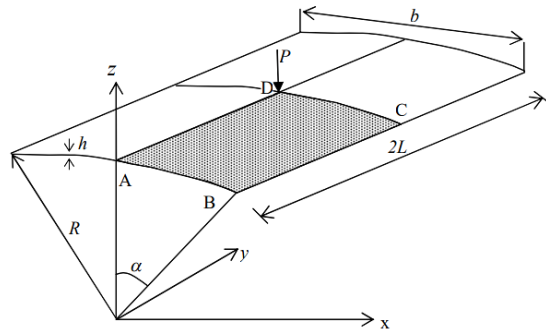


Figure 6. Example of cylindrical panel

Table 2. Geometrical and material properties

Properties	Symbol	Value
Radius	R	2.54 m
Thickness	e	6.35 mm
Height	H	25.4 m
Poisson ratio	$\nu$	0.3
Young modulus	E	3.103 GPa
Density	$\rho$	7800 Kg/m <sup>3</sup>

### 3. Results and Discussion

In our case, we will compare between our results and the existing results, then the analysis will be extended by using an elasto-plastic damage model according to Lemaitre's theory. After collecting all the data, we obtain the results illustrated and represented in the figures below for various values of the applied load.

In Figure 7. Multiple dynamic responses for various load values are overlaid for the purpose of analysing the obtained results. An initial observation reveals that when the load is equal to or less than  $N = 496$  N, the center displacement of the panel oscillates around the static displacement value  $W_c = 0.0076$  m, signifying stability in this scenario. However, at time  $t = 0.05$  s, a mere 1 N increase in the load leads to a sudden jump in the displacement, reaching nearly three and a half times the static value ( $W_c = 0.0270$  m). In this case, the critical load is determined to be  $N_{cr} = 497$  N, which agrees perfectly with the value found by Amieur et al. (2018) [16]  $N = 498$  N.

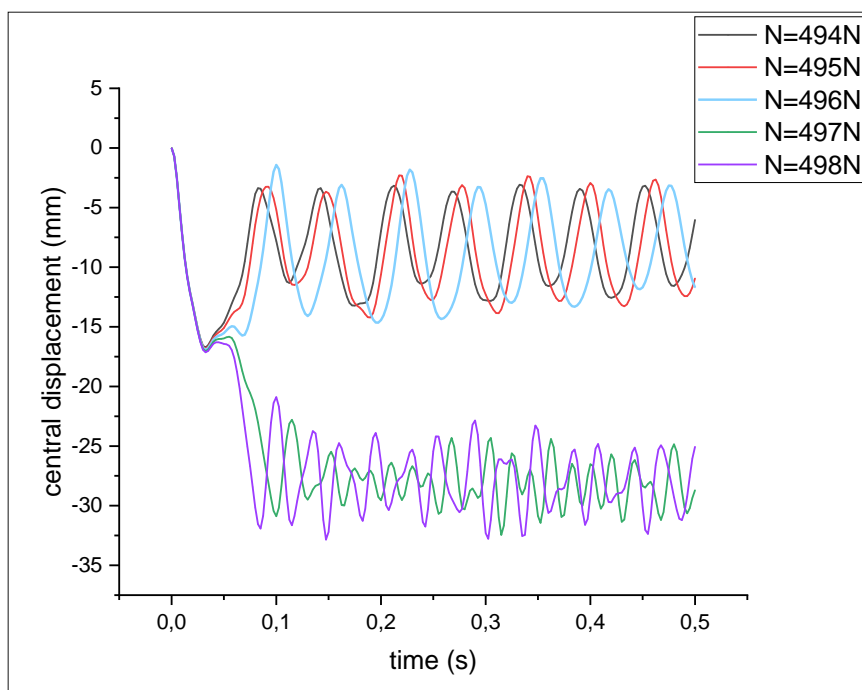


Figure 7. Determination of the critical load value ( $N_{cr}$ ) for elastic model

Furthermore, this value can also be ascertained using the phase plane criterion illustrated in Figures 8-a and 8-b. the structure oscillates around a displacement value corresponding to velocity equal zero for load values lower than  $N=496\text{N}$ , beyond this value and from the critical value of the load  $N = 497\text{N}$ , the trajectory makes an oscillation around this position before launching towards another equilibrium position.

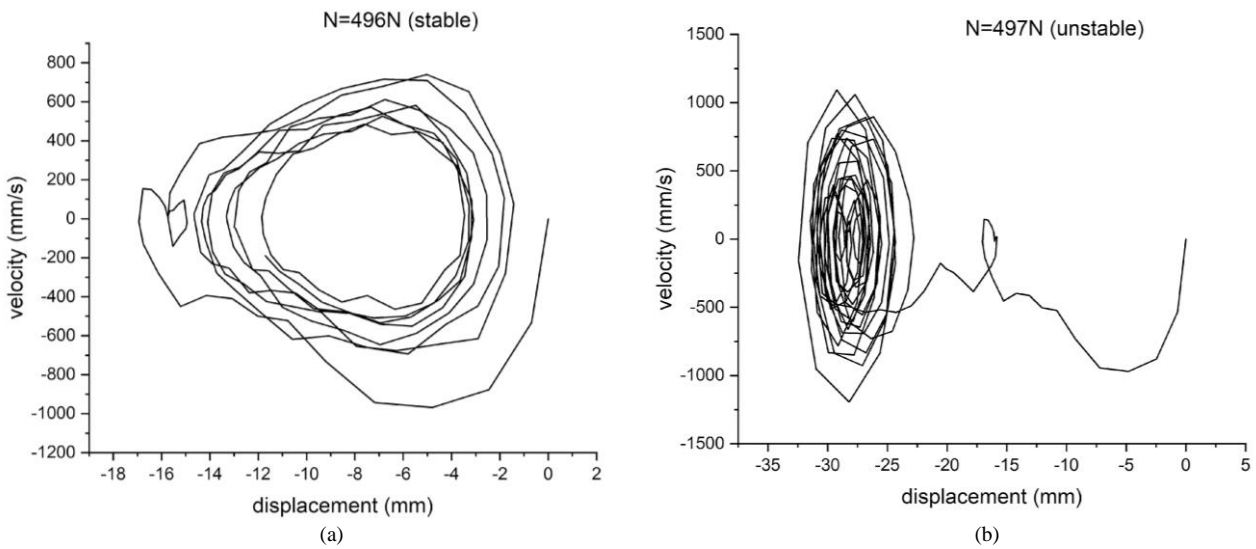


Figure 8. Phase plane diagram before and after the critical value for the elastic case

Figures 9 and 10 show the analysis as a function of the time of transverse displacement of the center of the panel, which is also the point of application of the concentrated force. Up to the value  $N=289\text{N}$ , the displacement gained is an oscillation around the position of the static balance. When the load  $N$  reaches  $290\text{N}$ , a dynamic bifurcation to another equilibrium position is recorded. The critical value of the dynamic bifurcation is therefore equal to  $290\text{N}$  for the von Mises criterion, while for Lemaitre’s model, we notice a slight decrease of  $7\text{N}$  between the two critical load values ( $N_{cr}$ ). The utilization of this model revealed dynamic buckling occurring earlier when compared to the von Mises criterion. We observed a shift from  $N = 290\text{N}$  to  $N = 283\text{N}$ .

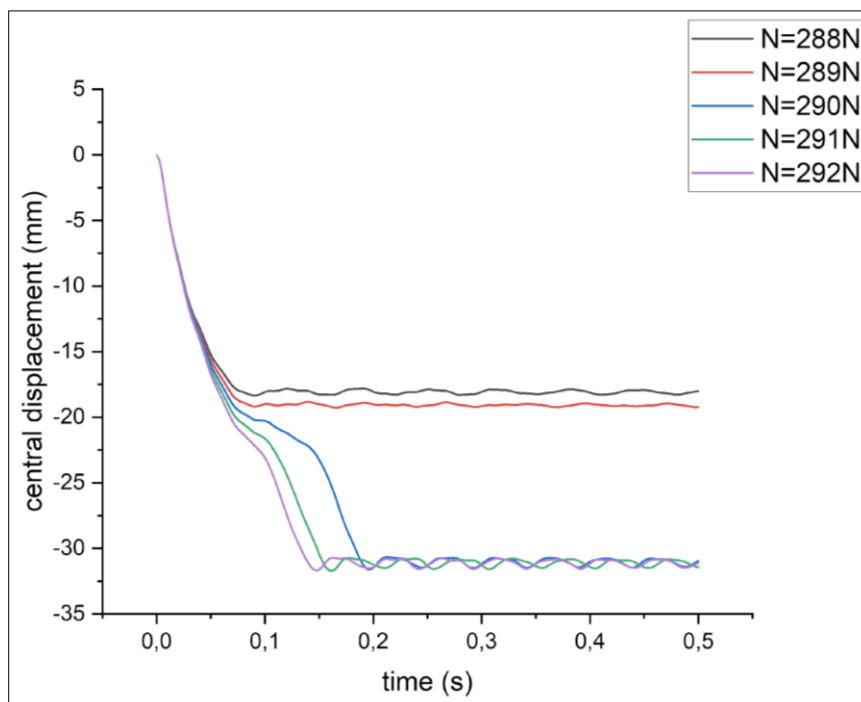
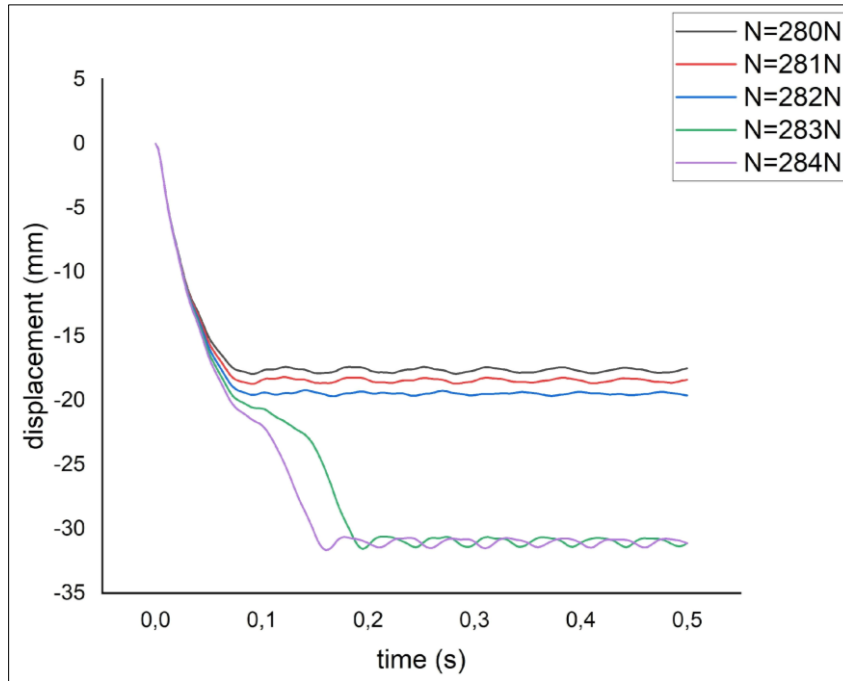
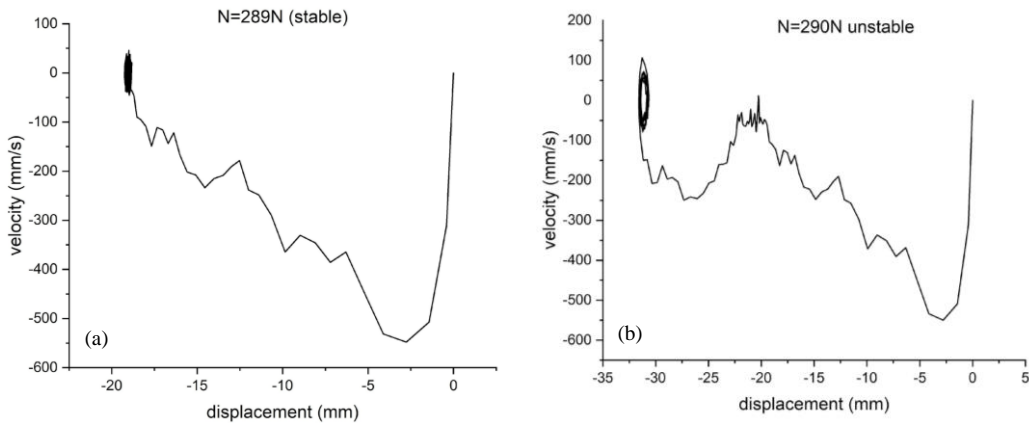


Figure 9. Determination of  $N_{cr}$  for von mises criterion



**Figure 10. Determination of  $N_{cr}$  for Lemaitre’s model**

The phase plane portraits (Figure 11) for the von-mises criterion corroborate this conclusion. Indeed, for  $N=289N$ , the trajectory of the movement is stable around the static equilibrium position (Figure 11-a). When  $N$  reaches the slightly higher value of  $290N$ , the trajectory makes some oscillations around this position before moving to another equilibrium position. The stable nature of this post-critical movement is clearly indicated in Figure 11-b. The same remarks were reported for the model of Lemaitre (Figures 12-a and 12-b) where for a value of  $N=282N$  the trajectory of the movement is stable around a value close to 18 mm. An increase of 1 N leads to a sudden jump in the displacement, reaching nearly 31 mm.



**Figure 11. Phase plane diagram before and after the critical value  $N_{cr}$  for van mises criterion**

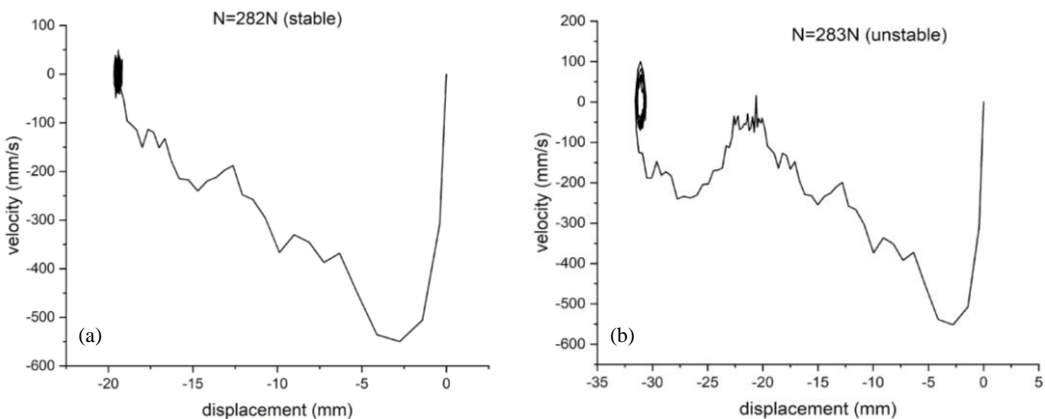


**Figure 12. Phase plane diagram before and after the critical value for Lemaitre’s model**

Figure 13 represents the variation of the damage parameter compared to time for the critical load in the previous example. We can divide the curve into three parts: the first part, where the damage  $D=0$  is defined for the elastic phase; the second part, where we note a considerable loss of the parameter of damage for booth value; and the last part, where all the gauss points reach the plasticity (a stabilization in the last part was noticed). We notice a considerable jump between the two values; we went from  $D = 0.15$  to  $D = 0.21$ .

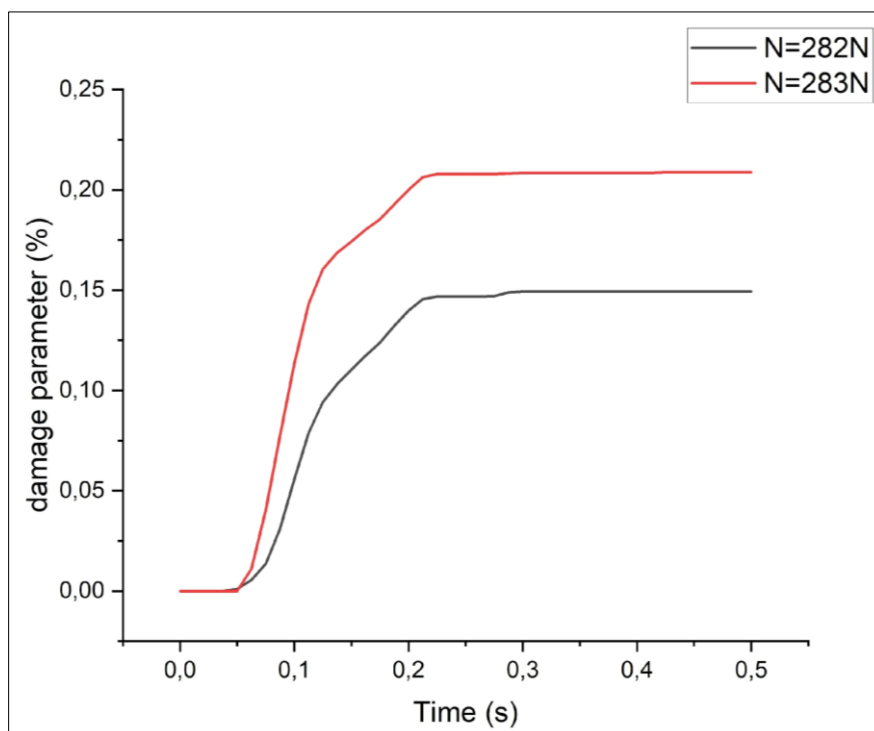


Figure 13. Damage parameter evolution of a cylindrical panel

## 4. Conclusion

Due to its significance in the industrial field, it has become more than necessary to discuss the stability of thin structures to optimize critical loads. In this article, an experimental methodology was used to identify the mechanical properties and damage parameters of thin shells, using the locally developed finite element program DYNCOQ to implement the Lemaitre model. The obtained results were initially compared to references in the literature cited in the first example to ensure the proper functioning of the program used and the good convergence of the damage model. Following this, the work was extended to study the dynamic buckling of thin shells using the equation of motion criterion and the phase plane criterion for determining the critical load. The experiment involved comparing both the von Mises plasticity criterion and the Lemaitre model. As a result, to conclude the research paper, first in the elastic plastic case, a noticeable decrease in the critical value compared to the elastic case is evident. There is also a slight decrease of 7N between the two plastic criteria, which is approximately a 10% loss. This value can go up to 15% if we calculate the damage parameter using the formula proposed by Lemaitre, and the final element is the minor 1 N increase in the load, which yields a substantial shift in the damage parameter values, transitioning from  $D = 0.15$  to  $D = 0.21$ .

## 5. Declarations

### 5.1. Author Contributions

Conceptualization, I.H., M.G., and B.A.; methodology, I.H., M.G., and B.A.; formal analysis, I.H., M.G., and B.A.; data curation, I.H., M.G., and B.A.; writing—original draft preparation, I.H., M.G., and B.A.; writing—review and editing, I.H., M.G., and B.A. All authors have read and agreed to the published version of the manuscript.

### 5.2. Data Availability Statement

The data presented in this study are available in the article.

### 5.3. Funding

This study was supported by FIMAS Laboratory, University of Tahri Mohamed Bechar, Algeria.

#### 5.4. Conflicts of Interest

The authors declare no conflict of interest.

#### 6. References

- [1] McClintock, F. A. (1968). A criterion for ductile fracture by the growth of holes. *Journal of Applied Mechanics, Transactions ASME*, 35(2), 363–371. doi:10.1115/1.3601204.
- [2] Gurson, A. L. (1977). Continuum theory of ductile rupture by void nucleation and growth: Part 1 - yield criteria and flow rules for porous ductile media. *Journal of Engineering Materials and Technology, Transactions of the ASME*, 99(1), 2–15. doi:10.1115/1.3443401.
- [3] Needleman, A., & Tvergaard, V. (1984). An analysis of ductile rupture in notched bars. *Journal of the Mechanics and Physics of Solids*, 32(6), 461–490. doi:10.1016/0022-5096(84)90031-0.
- [4] Lemaitre, J. (1985). A continuous damage mechanics model for ductile fracture. *Journal of Engineering Materials and Technology, Transactions of the ASME*, 107(1), 83–89. doi:10.1115/1.3225775.
- [5] Lee, S. W., Pourboghrat, F. (2005). A Simulation for the Punchless Piercing Process using Lemaitre Damage Model. *AIP Conference Proceedings*, 778, 505–510. doi:10.1063/1.2011271.
- [6] He, S., Wang, H., Bordas, S. P. A., & Yu, P. (2020). A Developed Damage Constitutive Model for Circular Steel Tubes of Reticulated Shells. *International Journal of Structural Stability and Dynamics*, 20(9). doi:10.1142/S0219455420501060.
- [7] Li, Y., Liu, Y., Mo, X., Shen, W., Li, C., Sun, X., & Xue, F. (2024). Damage evolution and fracture of aluminum alloy based on a modified Lemaitre model. *Engineering Fracture Mechanics*, 295, 109778. doi:10.1016/j.engfracmech.2023.109778.
- [8] Laboubi, S., Boussaid, O., Zaaf, M., & Ghennai, W. (2023). Numerical investigation and experimental validation of Lemaitre ductile damage model for DC04 steel and application to deep drawing process. *International Journal of Advanced Manufacturing Technology*, 126(5–6), 2283–2294. doi:10.1007/s00170-023-11244-0.
- [9] Anduquia-Restrepo, J., Narváez-Tovar, C., & Rodríguez-Baracaldo, R. (2018). Computational and numerical analysis of ductile damage evolution under a load-unload tensile test in dual-phase steel. *Journal of Mechanical Engineering*, 64(5), 339–348. doi:10.5545/sv-jme.2017.5137.
- [10] De Souza Neto, E. A. (2002). A fast, one-equation integration algorithm for the Lemaitre ductile damage model. *Communications in Numerical Methods in Engineering*, 18(8), 541–554. doi:10.1002/cnm.511.
- [11] Shamshiri, A. R., Haji Aboutalebi, F., & Poursina, M. (2023). Presenting an explicit step-by-step algorithm for lemaitre's ductile damage model with the crack closure effect in tensile-compressive loadings. *Mechanics Based Design of Structures and Machines*, 51(8), 4452–4466. doi:10.1080/15397734.2021.1966309.
- [12] Djermane, M. (2007). *Dynamic Buckling of Thin Shells in Seismic Zones*. Ph.D. Thesis, Houari-boumedièn University of Science and Technology, Bab Ezzouar, Algeria. (In French).
- [13] Djermane, M., Chelghoum, A., Amieur, B., & Labbaci, B. (2007). Nonlinear dynamic analysis of thin shells using a finite element with drilling degrees of freedom. *International Journal of Applied Engineering Research*, 2(1), 97–108.
- [14] Djermane, M., Zaoui, D., Labbaci, B., & Hammadi, F. (2014). Dynamic buckling of steel tanks under seismic excitation: Numerical evaluation of code provisions. *Engineering Structures*, 70, 181–196. doi:10.1016/j.engstruct.2014.03.037.
- [15] Belkacem, A. (2019). *Instability by dynamic buckling These Amieur 2018*. Ph.D. Thesis, Université Tahri Mohammed Béchar, Béchar, Algeria. (In French).
- [16] Amieur, B., Djermane, M., Zenkour, A. M., & Hammadi, F. (2023). Dynamic buckling analysis of functionally graded shells. *Mechanics Based Design of Structures and Machines*, 1–16. doi:10.1080/15397734.2023.2227886.
- [17] Dirichlet, P.G.L. (1846). Note II: On the Stability of the Equilibrium. *Works of Lagrange*, 11, 457–459.
- [18] Lyapunov, A. (1907). General problem of movement stability. *Annals of the Faculty of Sciences of Toulouse Mathematics*, 9, 203–474. doi:10.5802/afst.246.
- [19] Hoff, N. J., & Bruce, V. G. (1953). Dynamic Analysis of the Buckling of Laterally Loaded Flat Arches. *Journal of Mathematics and Physics*, 32(1–4), 276–288. doi:10.1002/sapm1953321276.
- [20] Simitses, G. (1966). Dynamic Snap-Through Buckling of Shallow Spherical Caps. *7<sup>th</sup> Structures and Materials Conference*. doi:10.2514/6.1966-1712.
- [21] Raftoyiannis, I. G., Constantakopoulos, T. G., Michaltsos, G. T., & Kounadis, A. N. (2006). Dynamic buckling of a simple geometrically imperfect frame using Catastrophe Theory. *International Journal of Mechanical Sciences*, 48(10), 1021–1030. doi:10.1016/j.ijmecsci.2006.05.010.

- [22] Bamberger Y. (1981). Disaster Theory and Elastic Stability of Structures. *Le Flambement des Structures L'Hermite*, 323–343.
- [23] Kounadis, A. N., & Raftoyiannis, J. (1990). Dynamic stability criteria of nonlinear elastic damped/undamped systems under step loading. *AIAA Journal*, 28(7), 1217–1223. doi:10.2514/3.25197.
- [24] Koimadis, A. N. (1991). Nonlinear dynamic buckling of discrete dissipative or non-dissipative systems under step loading. *AIAA Journal*, 29(2), 280–289. doi:10.2514/3.10575.
- [25] Kounadis, A. N. (1996). On the nonlinear dynamic buckling mechanism of autonomous dissipative/non-dissipative discrete structural systems. *Archive of Applied Mechanics*, 66(6), 395–408. doi:10.1007/bf00803674.
- [26] Kounadis, A. N., Gantes, C. J., & Bolotin, V. V. (1999). Dynamic buckling loads of autonomous potential systems based on the geometry of the energy surface. *International Journal of Engineering Science*, 37(12), 1611–1628. doi:10.1016/S0020-7225(98)00136-0.
- [27] Budiansky, B. (1962). Axisymmetric dynamic buckling of clamped shallow spherical shells. *NASA TN*, 1510, 597-606.
- [28] Budiansky, B. (1967). Dynamic Buckling of Elastic Structures: Criteria and Estimates. *Proceedings of an International Conference Held at Northwestern University, Evanston, Illinois*, 83-106. doi:10.1016/B978-1-4831-9821-7.50010-7.
- [29] Saigal, S., & Yang, T. Y. (1985). Nonlinear dynamic analysis with a 48 d.o.f. curved thin shell element. *International Journal for Numerical Methods in Engineering*, 21(6), 1115–1128. doi:10.1002/nme.1620210611.
- [30] Nagarajan, S., & Popov, E. P. (1974). Elastic-plastic dynamic analysis of axisymmetric solids. *Computers and Structures*, 4(6), 1117–1134. doi:10.1016/0045-7949(74)90028-5.
- [31] Bathe, K. J., Ramm, E., & Wilson, E. L. (1975). Finite element formulations for large deformation dynamic analysis. *International Journal for Numerical Methods in Engineering*, 9(2), 353–386. doi:10.1002/nme.1620090207.
- [32] Djermane, M., Chelghoum, A., Amieur, B., & Labbaci, B. (2007). Nonlinear dynamic analysis of thin shells using a finite element with drilling degrees of freedom. *International Journal of Applied Engineering Research*, 2(1), 97-108.